Beam-energy dependence of the azimuthal anisotropic flow from RHIC

Niseem Magdy (For the STAR Collaboration)[1, *]
[1] *Department of Physics, University of Illinois at Chicago, Chicago, Illinois 60607, USA*

Abstract: Recent STAR measurements of the anisotropic flow coefficients (v_n) are presented for Au+Au collisions spanning the beam energy range $\sqrt{s_{NN}} = 7.7 - 200$ GeV. The measurements indicate dependences on the harmonic number (n), transverse momentum (p_T), pseudorapidity (η), collision centrality and beam energy ($\sqrt{s_{NN}}$) which could serve as important constraints to test different initial-state models and to aid precision extraction of the temperature dependence of the specific shear viscosity.

Talk presented at the 2019 Meeting of the Division of Particles and Fields of the American Physical Society (DPF2019), July 29–August 2, 2019, Northeastern University, Boston, C1907293.

I. INTRODUCTION

A major aim of the heavy-ion experimental program at the Relativistic Heavy Ion Collider (RHIC) is to study the properties of the quark-gluon plasma (QGP) created in ion-ion collisions. Recently, several studies have highlighted the use of anisotropic flow measurements to investigate the transport properties of the QGP [1–7]. An essential question in many of these studies has been the role of initial-state fluctuations and their impact on the uncertainties associated with the extraction of η/s for the QGP [8, 9].

In this work, we present a new measurement for the anisotropic flow coefficients, $\mathrm{v}_n (n > 1)$ [10–12], and the rapidity-even dipolar flow coefficient, v_1^{even} [13, 14], with an eye toward providing a new constraint which could assist the distinction between different initial-state models and therefore, facilitate a more accurate extraction of the specific shear viscosity, η/s [15, 16].

The anisotropic flow is described by the coefficients, v_n, obtained from a Fourier expansion of the azimuthal angle (ϕ) distribution of the particles emitted in the collisions [17]:

$$\frac{dN}{d\phi} \propto 1 + 2\sum_{n=1} \mathrm{v_n} \cos(n(\phi - \Psi_n)), \quad (1)$$

where Ψ_n denotes the azimuthal angle of the n^{th}-order event plane; the coefficients, v_1, v_2 and v_3 define directed, elliptic, and triangular flow, respectively. The flow coefficients, v_n, are linked to the two-particle Fourier coefficients, $\mathrm{v}_{n,n}$, as:

$$\mathrm{v_{n,n}}(p_\mathrm{T}^a, p_\mathrm{T}^b) = \mathrm{v_n}(p_\mathrm{T}^a)\mathrm{v_n}(p_\mathrm{T}^b) + \delta_\mathrm{NF}, \quad (2)$$

where a and b are particles with p_T^a and p_T^b, respectively, and δ_NF is the non-flow (NF) term, which involves potential short-range contributions from resonance decays, Bose-Einstein correlation, near-side jets, and long-range contributions from the global momentum conservation (GMC) [18–20]. The short-range non-flow contributions can be reduced by applying a pseudorapidity gap, $\Delta\eta$, between η^a and η^b. However, the impacts of the GMC must be explicitly considered. For the current analysis, a simultaneous fitting method [13], outlined below, was used to account for the GMC.

II. MEASUREMENTS

The correlation function method was used to measure the two-particle $\Delta\phi$ correlations:

$$C_r(\Delta\phi, \Delta\eta) = \frac{(dN/d\Delta\phi)_{same}}{(dN/d\Delta\phi)_{mixed}}, \quad (3)$$

* niseemm@gmail.com

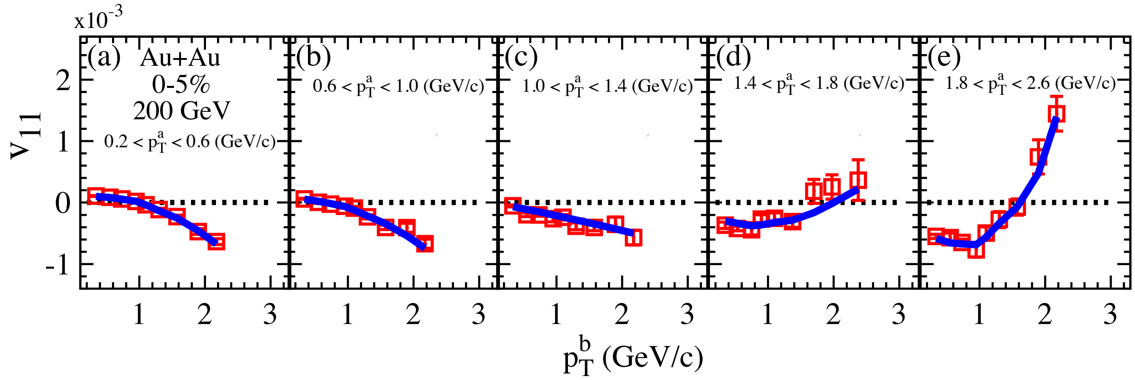

FIG. 1. $v_{1,1}$ vs. p_T^b for several selections of p_T^a for 0-5% central Au+Au collisions at $\sqrt{s_{NN}} = 200$ GeV. The dashed curves show the result of the simultaneous fit with Eq. 5. Figure are taking from Ref [13].

where $(dN/d\Delta\phi)_{same}$ denotes the normalized azimuthal distribution of particle pairs from the same event and $(dN/d\Delta\phi)_{mixed}$ denotes the normalized azimuthal distribution for particle pairs in which each member is selected from a different events but with a similar classification for the collision vertex location, centrality, etc. The pseudorapidity gap requirement $|\Delta\eta| > 0.7$ was applied to track pairs to reduce the non-flow contributions associated with the short-range correlations.

The two-particle Fourier coefficients, $v_{n,n}$, are extracted from the correlation function as:

$$\mathrm{v_{n,n}} = \frac{\sum_{\Delta\phi} C_r(\Delta\phi, \Delta\eta)\cos(n\Delta\phi)}{\sum_{\Delta\phi}\ C_r(\Delta\phi, \Delta\eta)}, \tag{4}$$

and then the two-particle Fourier coefficients, $v_{n,n}$, are used to extract v_1^{even} via a simultaneous fit of $v_{1,1}$ as a function of p_T^{b}, for several selections of p_T^a with Eq. 2:

$$\mathrm{v}_{1,1}(p_{\mathrm{T}}^a, p_{\mathrm{T}}^b) = \mathrm{v}_1^{\mathrm{even}}(p_{\mathrm{T}}^a)\mathrm{v}_1^{\mathrm{even}}(p_{\mathrm{T}}^b) - Cp_{\mathrm{T}}^a p_{\mathrm{T}}^b. \tag{5}$$

Here, $C \propto 1/(\langle Mult\rangle\langle p_T^2\rangle)$ takes into account the non-flow correlations caused by a global momentum conservation [20, 21] and $\langle Mult\rangle$ is the mean multiplicity. For a particular centrality selection, the left-hand side of Eq. 5 describes the $N \times N$ matrix which we fit with the right-hand side using $N + 1$ parameters; N values of $v_1^{even}(p_{\mathrm{T}})$ and one additional parameter C, accounting for the momentum conservation [22].

Figure 1 [13] shows the result of this fitting method for $0 - 5\%$ central Au+Au collisions at $\sqrt{s_{NN}} = 200$ GeV. The dashed curve (produced with Eq. 5) in each panel represents the effectiveness of the simultaneous fits, as well as the data constraining power. That is, $v_{1,1}(p_{\mathrm{T}}^b)$ grows from negative to positive values as the selection range for p_{T}^a is increased.

III. RESULTS

Representative set of STAR measurements for v_1^{even} and $v_n (n \geq 2)$ for Au+Au collisions at several different collision energies are summarized in Figs. 2, 3, 4 and 5.

The extracted values of $v_1^{even}(p_{\mathrm{T}})$ for 0-10%, 10-20% and 20-30% centrality selections are shown in Fig. 2; the solid line in panel (a) indicates the hydrodynamic calculations [21], that in good agreement with our measurements, the inset displays the results of the associated momentum conservation coefficient, C, obtained for several centralities at $\sqrt{s_{NN}} = 200$ GeV. The $v_1^{even}(p_{\mathrm{T}})$ values show the characteristic pattern of a change from negative $v_1^{even}(p_{\mathrm{T}})$ at low p_{T} to positive $v_1^{even}(p_{\mathrm{T}})$ for $p_{\mathrm{T}} > 1$ GeV/c, with a crossing point that slowly shifts with $\sqrt{s_{NN}}$. They also indicate that v_1^{even} increases as the collisions become more peripheral, as might be expected from the centrality dependence of ε_1.

Figure 2 shows the p_T dependence of the $v_n (n \geq 2)$ measurements for 0-40% centrality selection for a representative set of beam energies. Fig. 2 shows the v_n dependence on p_T and the harmonic number, n, with similar trends for each beam energy.

The centrality dependence of $v_n (n \geq 2)$ is indicated in Fig. 4 for the same representative set of beam energies. Our measurements indicate a soft centrality dependence for the higher-order flow harmonics,

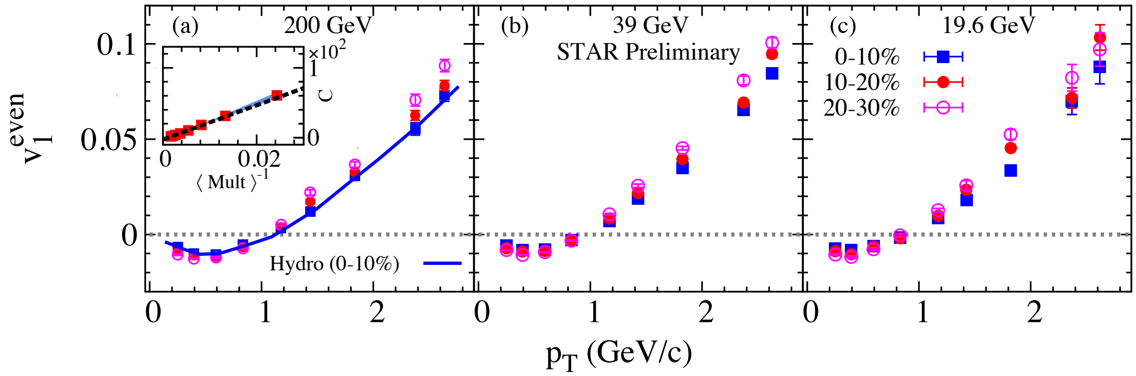

FIG. 2. The extracted values of v_1^{even} vs. p_T for different centrality selections (0-10%, 10-20% and 20-30%) of Au+Au collisions for several values of $\sqrt{s_{NN}}$. The v_1^{even} values are obtained via fits with Eq. (5). The solid line in panel (a) shows the result from a hydrodynamic calculations with $\eta/s = 0.16$ [21]. The inset in panel (a) shows a representative set of the associated values of C vs. the corrected mean multiplicity for $|\eta| < 0.5$ ($\langle Mult\rangle^{-1}$). The extracted v_1^{even} for $\sqrt{s_{NN}} = 200$, 39 and 19.6 GeV are shown in panels a, b and c respectively.

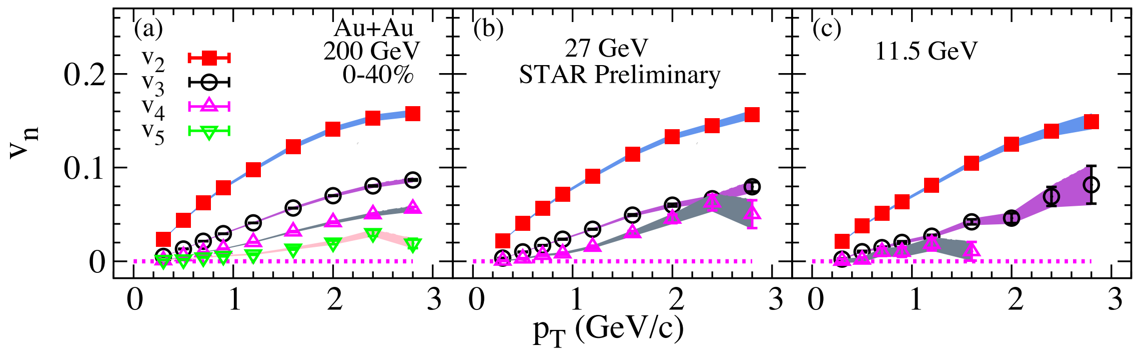

FIG. 3. The $v_n(p_T)$ as a function of p_T for charged particles in 0-40% central Au+Au collisions. The shaded bands represent the systematic uncertainty. The measured $v_n(p_T)$ for $\sqrt{s_{NN}} = 200$, 27 and 11.5 GeV are shown in panels a, b and c respectively.

which all decrease with decreasing the $\sqrt{s_{\rm NN}}$. These v_n patterns may be related to the dependence of the viscous effects in the created medium, which lead to attenuation of v_n magnitude.

Figure 5 gives the excitation functions for the p_T-integrated v_2, v_3 and v_4 for $0-40\%$ central Au+Au collisions. They indicate monotonic trend for v_n with $\sqrt{s_{\rm NN}}$, as might be expected for a temperature increase with $\sqrt{s_{\rm NN}}$.

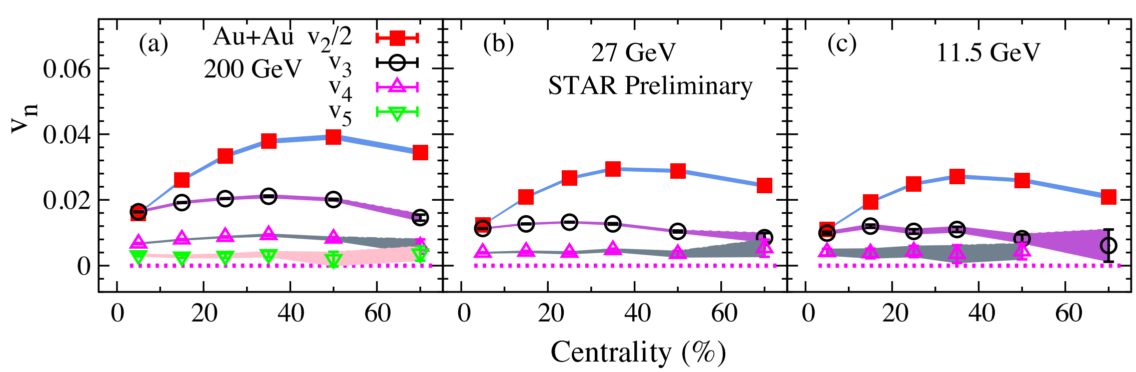

FIG. 4. The v_n as a function of Au+Au collision centrality for charged particles with $0.2 < p_T < 4$ GeV/c. The shaded bands represent the systematic uncertainty. The measured v_n(Centrality%) for $\sqrt{s_{NN}} = 200$, 27 and 11.5 GeV are shown in panels a, b and c respectively.

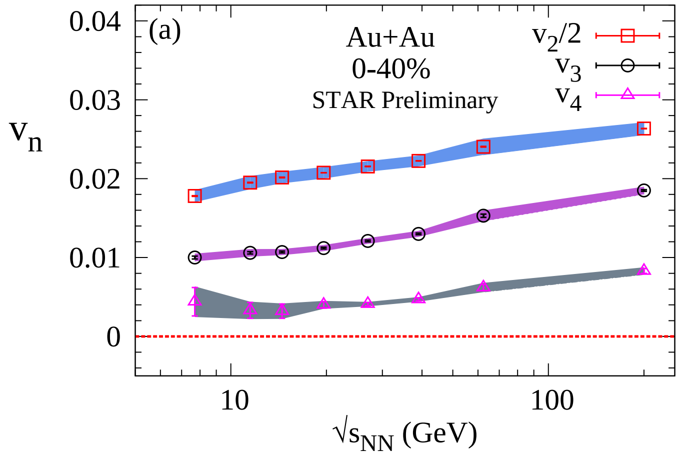

FIG. 5. The $v_n(\sqrt{s_{NN}})$ for charged particles with $0.2 < p_T < 4$ GeV/c and 0-40% central Au+Au collisions. The shaded bands represent the systematic uncertainty. The dashed line at $v_n = 0$ is to guide the eye.

IV. CONCLUSION

In summary, we have presented a comprehensive set of STAR anisotropic flow measurements for Au+Au collisions at $\sqrt{s_{NN}}$ = 7.7-200 GeV. The measurements use the two-particle correlation method to obtain the Fourier coefficients, $v_n(n > 1)$, and the rapidity-even dipolar flow coefficient, v_1^{even}. The rapidity-even dipolar flow measurements indicate the characteristic patterns of an evolution from negative $v_1^{even}(p_T)$ for $p_T < 1$ GeV/c to positive $v_1^{even}(p_T)$ for $p_T > 1$ GeV/c, expected when initial-state geometric fluctuations act along with the hydrodynamic-like expansion to generate rapidity-even dipolar flow. The $v_n(n > 1)$ measurements show a rich set of dependences on harmonic number n, p_T and centrality for several collision energies. This set of measurements may provide additional constraints to test different initial-state models and to aid accuracy extraction of the temperature dependence of the specific shear viscosity.

ACKNOWLEDGMENTS

This research is supported by the US Department of Energy under contract DE-FG02-94ER40865.

[1] D. Teaney, Phys.Rev. **C68**, 034913 (2003), arXiv:nucl-th/0301099 [nucl-th].
[2] R. A. Lacey and A. Taranenko, PoS **CFRNC2006**, 021 (2006), arXiv:nucl-ex/0610029 [nucl-ex].
[3] B. Schenke, S. Jeon, and C. Gale, Phys.Lett. **B702**, 59 (2011), arXiv:1102.0575 [hep-ph].
[4] H. Song, S. A. Bass, and U. Heinz, Phys.Rev. **C83**, 054912 (2011), arXiv:1103.2380 [nucl-th].
[5] H. Niemi, G. Denicol, P. Huovinen, E. Molnar, and D. Rischke, Phys.Rev. **C86**, 014909 (2012), arXiv:1203.2452 [nucl-th].
[6] G.-Y. Qin, H. Petersen, S. A. Bass, and B. Muller, Phys.Rev. **C82**, 064903 (2010), arXiv:1009.1847 [nucl-th].
[7] N. Magdy (STAR), *Proceedings, 16th International Conference on Strangeness in Quark Matter (SQM 2016): Berkeley, California, United States*, J. Phys. Conf. Ser. **779**, 012060 (2017).
[8] B. Alver and G. Roland, Phys. Rev. **C81**, 054905 (2010), [Erratum: Phys. Rev.C82,039903(2010)], arXiv:1003.0194 [nucl-th].
[9] R. A. Lacey, D. Reynolds, A. Taranenko, N. N. Ajitanand, J. M. Alexander, F.-H. Liu, Y. Gu, and A. Mwai, J. Phys. **G43**, 10LT01 (2016), arXiv:1311.1728 [nucl-ex].
[10] N. Magdy (STAR), *Proceedings, 27th International Conference on Ultrarelativistic Nucleus-Nucleus Collisions (Quark Matter 2018): Venice, Italy, May 14-19, 2018*, Nucl. Phys. **A982**, 255 (2019), arXiv:1807.07638 [nucl-ex].
[11] J. Adam *et al.* (STAR), Phys. Rev. Lett. **122**, 172301 (2019), arXiv:1901.08155 [nucl-ex].

[12] N. Magdy (STAR), *Proceedings, 11th International Workshop on Critical Point and Onset of Deconfinement (CPOD2017): Stony Brook, NY, USA, August 7-11, 2017*, PoS **CPOD2017**, 005 (2018), arXiv:1801.07872 [nucl-ex].
[13] J. Adam *et al.* (STAR), Phys. Lett. **B784**, 26 (2018), arXiv:1804.08647 [nucl-ex].
[14] N. Magdy (STAR), *EPJ Web of Conferences 171, 16002 (2018)*, EPJ Web Conf. **171**, 16002 (2018), arXiv:1802.03869 [nucl-ex].
[15] J. Auvinen, I. Karpenko, J. E. Bernhard, and S. A. Bass, (2017), arXiv:1706.03666 [hep-ph].
[16] J. Auvinen, I. Karpenko, J. E. Bernhard, and S. A. Bass, *Proceedings, 26th International Conference on Ultra-relativistic Nucleus-Nucleus Collisions (Quark Matter 2017): Chicago, Illinois, USA, February 5-11, 2017*, Nucl. Phys. **A967**, 784 (2017), arXiv:1704.04643 [nucl-th].
[17] A. M. Poskanzer and S. A. Voloshin, Phys. Rev. **C58**, 1671 (1998), arXiv:nucl-ex/9805001 [nucl-ex].
[18] R. A. Lacey, *Proceedings, 18th International Conference on Ultra-Relativistic Nucleus-Nucleus Collisions (Quark Matter 2005): Budapest, Hungary, August 4-9, 2005*, Nucl. Phys. **A774**, 199 (2006), arXiv:nucl-ex/0510029 [nucl-ex].
[19] N. Borghini, P. M. Dinh, and J.-Y. Ollitrault, Phys. Rev. **C62**, 034902 (2000), arXiv:nucl-th/0004026 [nucl-th].
[20] G. Aad *et al.* (ATLAS), Phys. Rev. **C86**, 014907 (2012), arXiv:1203.3087 [hep-ex].
[21] E. Retinskaya, M. Luzum, and J.-Y. Ollitrault, Phys. Rev. Lett. **108**, 252302 (2012), arXiv:1203.0931 [nucl-th].
[22] J. Jia, S. K. Radhakrishnan, and S. Mohapatra, J. Phys. **G40**, 105108 (2013), arXiv:1203.3410 [nucl-th].